ANESTHESIOLOGY

Gas Phase Diffusion Does Not Limit Lung Volatile Anesthetic Uptake Rate

Philip J. Peyton, M.D., Ph.D., M.B.B.S., F.A.N.Z.C.A.

ANESTHESIOLOGY 2022; 137:176–86

EDITOR'S PERSPECTIVE

What We Already Know about This Topic

- Inefficiency of gas uptake and elimination in the lung is reflected by development of partial pressure gradients between expired alveolar (end-tidal) gas and arterial blood
- These arise mainly from variation of alveolar ventilation–perfusion ratios across the lung, but longitudinal partial pressure gradients down the respiratory tree due to diffusion limitation may possibly also contribute, especially for larger molecules such as volatile anesthetics

What This Article Tells Us That Is New

- The hypothesis that the end-tidal to arterial partial pressure gradient for desflurane would be larger than that for nitrous oxide was tested in 17 patients inhaling a mixture of desflurane and nitrous oxide, which have similar effective blood–gas partition coefficients but a fourfold difference in molecular weight
- Raw measurements of end-tidal to arterial partial pressure gradients, relative to inspired concentration, were smaller for desflurane
- After adjustment for the higher rate of lung gas uptake for desflurane at the time of measurement, no difference was found in end-tidal to arterial partial pressure gradients

ABSTRACT

Background: Inefficiency of lung gas exchange during general anesthesia is reflected in alveolar (end-tidal) to arterial (end-tidal–arterial) partial pressure gradients for inhaled gases, resulting in an increase in alveolar deadspace. Ventilation–perfusion mismatch is the main contributor to this, but it is unclear what contribution arises from diffusion limitation in the gas phase down the respiratory tree (longitudinal stratification) or at the alveolar–capillary barrier, especially for gases of high molecular weight such as volatile anesthetics.

Methods: The contribution of longitudinal stratification was examined by comparison of end-tidal–arterial partial pressure gradients for two inhaled gases with similar blood solubility but different molecular weights: desflurane and nitrous oxide, administered together at 2 to 3% and 10 to 15% inspired concentration (FIG), respectively, in 17 anesthetized ventilated patients undergoing cardiac surgery before cardiopulmonary bypass. Simultaneous measurements were done of tidal gas concentrations, of arterial and mixed venous blood partial pressures by headspace equilibration, and of gas uptake rate calculated using the direct Fick method using thermodilution cardiac output measurement. Adjustment for differences between the two gases in FIG and in lung uptake rate (VG) was made on mass balance principles. A 20% larger end-tidal–arterial partial pressure gradient relative to inspired concentration (PETG – PaG)/FIG for desflurane than for N_2O was hypothesized as physiologically significant.

Results: Mean (SD) measured (PETG – PaG)/FIG for desflurane was significantly smaller than that for N_2O (0.86 [0.37] *vs.* 1.65 [0.58] mmHg; $P < 0.0001$), as was alveolar deadspace for desflurane. After adjustment for the different VG of the two gases, the adjusted (PETG – PaG)/FIG for desflurane remained less than the 20% threshold above that for N_2O (1.62 [0.61] *vs.* 1.98 [0.69] mmHg; $P = 0.028$).

Conclusions: No evidence was found in measured end-tidal to arterial partial pressure gradients and alveolar deadspace to support a clinically significant additional diffusion limitation to lung uptake of desflurane relative to nitrous oxide.

(ANESTHESIOLOGY 2022; 137:176–86)

Inefficiency of gas uptake and elimination in the lung is reflected by the development of measurable partial pressure gradients between expired alveolar (end-tidal) gas and arterial blood (end-tidal–arterial partial pressure gradients). Both "parallel" and "longitudinal" inhomogeneity in gas exchange throughout the lung may contribute to end-tidal–arterial partial pressure gradients.[1] Parallel inhomogeneity is variation of alveolar ventilation–perfusion ratios throughout the lung ($\dot{V}_A / \dot{Q}$ scatter), which becomes significant under general anesthesia even in patients with normal lung function.[2–7] Longitudinal or "stratified" inhomogeneity refers to the development of partial pressure gradients down the respiratory tree and is largely due to diffusion limitation. This is expected to be more prominent for gases of high molecular weight and may occur both across the alveolar capillary membrane and in the gas phase in conducting airways, where it is governed by Graham's law and the square root of molecular weight.[8–10]

End-tidal to arterial partial pressure gradients for volatile anesthetics are typically between 15 and 30% of measured end-tidal partial pressure.[11,12] Furthermore, the alveolar

This article is featured in "This Month in Anesthesiology," page A1. This article has a visual abstract available in the online version.

Submitted for publication January 6, 2022. Accepted for publication April 25, 2022. Published online first on May 3, 2022.

Philip J. Peyton, M.D., Ph.D., M.B.B.S., F.A.N.Z.C.A.: Department of Critical Care, Melbourne Medical School, Faculty of Medicine Dentistry and Health Sciences, University of Melbourne, Victoria, Australia; Department of Anesthesia, Austin Health, Heidelberg, Victoria, Australia; and Institute for Breathing And Sleep, Heidelberg, Victoria, Australia.

 Anesthesiology 2022; 137:176–86. DOI: 10.1097/ALN.0000000000004260

deadspace for volatile anesthetics is two to three times larger than that measured simultaneously for carbon dioxide in anesthetized ventilated patients and is inversely related to the solubility of the anesthetic in blood.[11,12] Modeling of physiologically realistic $\dot{V}_A / \dot{Q}$ distributions across the lung shows how this difference is predominantly driven by $\dot{V}_A / \dot{Q}$ scatter, which generates different end-tidal–arterial partial pressure gradients for gases of different solubilities. However, given the high molecular weight of these gases, diffusion limitation remains a possible factor contributing to end-tidal–arterial partial pressure gradients and alveolar deadspace for these anesthetics.[12] While this possibility was suggested almost 30 yr ago, it has received no investigation for volatile anesthetics since.[11]

A potential physiologic model for distinguishing the contributions of $\dot{V}_A / \dot{Q}$ scatter and gas phase diffusion limitation to lung gas exchange inefficiency is simultaneous comparison of the end-tidal–arterial partial pressure gradients for two inhaled gases with similar blood solubility but different molecular weights, such as the anesthetics desflurane (molecular weight, 168) and N_2O (molecular weight, 44). While controlling for the effects on end-tidal and arterial partial pressures of differences in (1) inspired concentration and (2) blood solubility of the two gases, such a comparison also needs to compensate for the effect of (3) any difference between them in the rate of lung gas uptake at the time of measurement. It was hypothesized that, after adjustment for these three factors, the end-tidal–arterial partial pressure gradient for desflurane would be greater than that for nitrous oxide. This study was done in anesthetized, ventilated patients undergoing precardiopulmonary bypass cardiac surgery.

Material and Methods

With approval by the local institutional ethics review committee (HREC/16/Austin/419, amendment December 10, 2019) and with informed written individual consent, adult patients scheduled to undergo elective cardiac surgery at the Austin Hospital (Melbourne, Australia), were recruited to the study (registered in the Australian and New Zealand Clinical Trials Registry, No. 373206). Patients were deemed eligible for recruitment to this observational study if they had no history of lung disease preoperatively or if routine preoperative lung function testing showed a forced expiratory volume in one second (FEV_1) and forced vital capacity (FVC) greater than 50% of predicted for body size, and a FEV_1/FVC ratio of at least 50%.

Anesthesia management consisted of routine patient cardiovascular monitoring with peripheral arterial and pulmonary artery catheters, along with continuous tidal gas concentration monitoring and arterial and mixed venous blood–gas analysis in the precardiopulmonary bypass period. After intravenous induction of anesthesia with propofol, opioid, and nondepolarizing neuromuscular blocker and tracheal intubation, the patient was connected to a circle breathing system on a Zeus anesthetic machine (Drägerwerk AG, Germany) with fresh carbon dioxide absorber to eliminate carbon dioxide rebreathing. Tidal volume was set at 7 to 10 ml/kg with 5 cm H_2O positive end-expiratory pressure, and the respiratory rate was set so as to achieve an end-tidal carbon dioxide partial pressure (P_{ETCO_2}) of 25 to 35 mmHg with further adjustment after arterial blood sampling to target normocapnia, with an inspired to expired (I:E) ratio that ensured a smooth and flat phase 3 plateau on the capnogram.

After commencement of ventilation, delivery of an inhaled mixture of desflurane and nitrous oxide was commenced at a fresh gas flow rate of at least 6 l/min with balance fresh gas oxygen and with supplementary intravenous propofol infusion and opioid to maintain adequate depth of anesthesia guided by processed electroencephalograph monitoring. On achievement of near steady-state maintenance phase inhalational anesthesia, between 30 and 60 min postinduction of anesthesia and before cardiopulmonary bypass, and during a period of stability (less than 10% change over at least a 5-min period of time) in ventilation settings, heart rate, mean arterial blood pressure, and end-expired concentration of carbon dioxide and desflurane and nitrous oxide, data and sample collection was performed by the investigator. This consisted of cardiac output measured by right heart thermodilution (average of three consecutive measurements) and collection of simultaneous paired arterial and mixed venous blood samples, along with recording of inspired and end-tidal concentrations of oxygen, carbon dioxide, and desflurane and nitrous oxide by side-stream gas sampling by the gas analyzer. Simultaneous blood samples were also processed for measurement of respiratory blood gases on the ABL 800 gas analyzer (Radiometer, Denmark) calibrated according to the manufacturer's specifications.

In all patients, the delivered concentrations of the two study gases (G) were 2 to 3% desflurane and 10 to 15% N_2O, with balance gas oxygen. These values were chosen to achieve inspired concentrations (F_IG) and partial pressures in blood samples for each gas that were well within the dynamic measurement range of the gas analyzer. This was a Datex–Ohmeda Capnomac Ultima (GE Healthcare, USA), which has a dynamic reference range (0 to 10 V) of 0 to 20% for desflurane and 0 to 100% for N_2O. This was connected to a notebook computer (Macbook Air, Apple Corp, USA) running LabVIEW 2011 software (National Instruments, USA) *via* an analog–digital converter card (USB 6009, National Instruments) to allow real time capture on hard disk of all raw gas concentration data. The linearity of the gas analyzer for both gases was confirmed by construction of calibration curves using a stock mixture of desflurane and nitrous oxide encompassing the range of partial pressures encountered in the study using 8-fold serial 50% dilutions of a prepared mixture of both gases in oxygen.

Partial pressures for desflurane and nitrous oxide in arterial and mixed venous blood were measured by gas analysis after equilibration with 10 ml of headspace gas in heparinized gas-tight glass syringes in a shaking water bath at body temperature. Headspace gas analysis was performed by the same infrared gas analyzer as used to measure tidal gas concentrations, using a method previously described, which avoids calibration errors that can occur when devices (such as chromatographs) different from those used for tidal gas sampling are used to measure gas content in blood.[13] The infrared rapid gas analyzer had 10 to 90% response times of approximately 360 ms, allowing accurate measurement of end inspired and expired gas partial pressures in tidal gas sampling at the respiratory frequencies used (10 to 14 breaths/min) and of headspace gas sampling for measurement in blood samples. All measured partial pressures were corrected to body temperature, pressure, and water vapor saturated. The sampling process therefore provided simultaneous measurements for each gas (G) of inspired (PIG), end-tidal (PETG), mixed venous ($P\bar{v}G$), and arterial (PaG) partial pressures, and therefore of the end-tidal–arterial partial pressure gradient (PETG – PaG).

The blood–gas partition coefficients at body temperature λG for desflurane and N_2O were individually measured in each patient by double headspace equilibration of the arterial blood sample with a mixture of 10% desflurane and 50% N_2O in oxygen. Given the different FIG for the two gases, comparison of λG for desflurane and N_2O was done using the effective λG, *i.e.*, λG×(1 – FIG), which adjusts for the difference between inspired and expired alveolar ventilation rates in calculations of lung gas uptake and is the most appropriate and precise value to use in the setting of a constant outflow model of inert gas uptake such as the calculation of alveolar deadspace for these gases is based upon.[14,15]

Calculations and Endpoints

Measurement of simultaneous gas partial pressures and content in arterial and mixed venous blood and inspired and end-tidal (mixed alveolar) gas for desflurane, nitrous oxide, oxygen, and carbon dioxide allowed calculation of lung uptake and elimination rates for all gases and shunt fraction and of alveolar deadspace fraction for CO_2 (V_{DA}/V_{ACO_2}) and for each anesthetic gas (V_{DA}/V_{AG}). The equations used for these calculations are given in the Appendix. Because FIG was low for both desflurane and nitrous oxide, for comparison of the two gases, FIG was treated as a simple scaling factor to the partial pressures measured. Statistical comparisons of measured, predicted, and adjusted partial pressures of desflurane with nitrous oxide partial pressures were therefore all done using values scaled according to FIG of each gas: *e.g.,* (PETG – PaG)/FIG.

The preplanned statistical analysis plan stipulated the primary endpoint to be comparison of (PETG – PaG)/FIG of desflurane with that of N_2O. V_{DA}/V_{AG} for the two gases was compared as a secondary endpoint. Patients acted as their own controls because both gases were being delivered and sampled simultaneously in each patient. Using data from our previous study measuring V_{DA}/V_{AG} for several volatile anesthetics, including desflurane, in a similar population, a mean V_{DA}/V_{AG} for desflurane of 0.65 was expected, with an observed SD of 0.10 in the difference in V_{DA}/V_{AG} between simultaneously measured gases. It was hypothesized that V_{DA}/V_{AG} for desflurane would be at least 10% (relative) larger than that for N_2O in the study population, due to diffusion limitation. This would correspond to an approximately 20% difference in end-tidal–arterial partial pressure gradient (scaled by inspired partial pressure), which was arbitrarily considered to be a physiologically significant difference. To provide 80% power to demonstrate this difference with a two-way type 1 error rate of 5%, data from 19 patients was required. Ethics committee approval for recruitment of 20 patients for this study was obtained.

Effect of Differences in Lung Uptake Rate

Interim analysis of the data from the first six patients indicated that different rates of lung uptake ($\dot{V}G$) between desflurane and N_2O was an additional factor having a substantial influence on the measurements of (PETG – PaG)/FIG and V_{DA}/V_{AG}. Despite having identical blood–gas partition coefficients, even if delivered at identical inspired concentration, desflurane and nitrous oxide are expected to have different rates of lung uptake due to differences in peripheral uptake driven by differences in solubility in body tissues, particularly in muscle and fat stores.[16] This is expected to affect the equilibration partial pressure of each gas in any given lung compartment and therefore to affect end-tidal partial pressure (PETG), arterial partial pressure (PaG), and thus (PETG – PaG)/FIG and V_{DA}/V_{AG}. The mathematical basis for this effect is outlined in the appendix, based on simple mass balance of lung gas exchange for a gas (G). The equations include a diffusion barrier for gas (G), creating a partial pressure difference (ΔPDG) between alveolar gas (PaG) and end-tidal gas (PETG), which is assumed to be 0 for N_2O in the study.

Equation 1 shows that for two gases with an identical end-tidal–arterial partial pressure gradient administered simultaneously to a subject at a given FIG, $\dot{V}A$, $\dot{V}O_2$, and $\dot{V}CO_2$, the measured alveolar deadspace is expected to be smaller for the gas with a higher $\dot{V}G$.

$$V_{DA}/V_{AG} = \frac{P_{ETG} - PaG}{\frac{\dot{V}G \times (PB - PIG) - (\dot{V}O_2 - \dot{V}CO_2) \times PIG}{\dot{V}A} + P_{ETG} - PaG} \quad \text{Equation 1}$$

Similarly, equation 2 indicates that where a gas is administered at a given FIG in the presence of a given $P\bar{v}G$, the effect of an increase in $\dot{V}G$ is to narrow the difference between PETG and PaG.

$$(P_{ET}G - PaG)/FIG = PB \times \left(1 + \frac{\dot{V}O_2 - \dot{V}CO_2}{\dot{V}A}\right) - \frac{P\bar{v}G}{FIG} - \frac{PB \times \dot{V}G}{FIG} \times \left(\frac{\dot{V}A + \dot{Q}t \times \lambda G \times (1-FIG)}{\dot{V}A \times \dot{Q}t. \times \lambda G}\right) \quad \text{Equation 2}$$

The slope of the relationship of $\dot{V}G$ to $(P_{ET}G - PaG)/FIG$ can be obtained by differentiation of equation 2, treating the other variables as independent.

$$\frac{d(P_{ET}G - PaG)/FIG}{d\dot{V}G/FIG} = -PB \times \left(\frac{\dot{V}A + \dot{Q}t \times \lambda G \times (1 - FIG)}{\dot{V}A \times \dot{Q}t. \times \lambda G}\right) \quad \text{Equation 3}$$

The effect of differences in measured $\dot{V}G$ on the comparison of the measured $(P_{ET}G - PaG)/FIG$ for desflurane and N_2O was estimated by equation 3, using the measured values for $\dot{V}A$, $\dot{Q}t$, FIG, λG, and the mean of $\dot{V}G$ measured in blood and gas phases in each patient. This was used to estimate an adjusted value for $(P_{ET}G - PaG)/FIG$ for desflurane for comparison with the hypothesized physiologic significance threshold of 20% above the mean measured $(P_{ET}G - PaG)/FIG$ for N_2O.

Statistical Analyses

Comparison of mean values and differences with the *t* test for paired data was done where distributions of data were consistent with a normal distribution according to the Shapiro–Wilk test, reporting SD, or 95% CI. Otherwise median values and interquartile range were compared using nonparametric statistical tests (Kruskal–Wallis equality-of-populations rank test). All statistical comparisons were two-tailed, with a threshold of significance of $P < 0.05$, and analysis was done using Stata 12 (StataCorp, USA).

Results

A total of 20 patients were recruited to the study, in 17 of whom (15 males and 2 females) complete data was able to be collected. In two patients, interruption of ventilation during the blood sampling process occurred due to surgical necessity associated with mammary artery graft harvesting, and in one patient, arterial blood headspace gas sample analysis was disrupted by automatic recalibration of the gas analyzer during introduction of the sample, resulting in their exclusion from the final data analysis. Data collection took place at a median [interquartile range] of 40 [35, 45] min after commencement of administration of the inspired gas mixture. Table 1 shows the physiologic data for the 17 patients, including measured $V_D/V_T CO_2$, $\dot{Q}s/\dot{Q}t$, and $\dot{V}O_2$ and $\dot{V}CO_2$ measured in blood by the Fick method.

Table 2 shows the measured values for the inspired concentration (FIG), alveolar or end-tidal ($P_{ET}G/FIG$), arterial (PaG/FIG), and mixed venous ($P\bar{v}G/FIG$) partial pressures scaled by FIG, and the end-tidal–arterial partial pressure difference $(P_{ET}G - PaG)/FIG$. The measured effective λG values were similar for the two gases. $P_{ET}G/FIG$ for desflurane was lower than that for N_2O and similar to previously published data.[16] The rate of lung gas uptake $\dot{V}G/FIG$, calculated in the both blood (equation A5) and gas (equation A8) phases are given in table 2. For both gases, there were no significant differences between these values for $\dot{V}G/FIG$. For desflurane median [interquartile range] $\dot{V}G/FIG$ was 4.4 [3.5, 5.0] ml/min in the blood phase and 3.9 [3.6, 5.1] ml/min in the gas phase ($P = 0.877$). For N_2O, $\dot{V}G/FIG$ was 3.3 [1.9, 4.2] ml/min in the blood phase and 2.7 [2.4, 3.3] ml/min in the gas phase ($P = 0.804$). $\dot{V}G/FIG$ was significantly higher for desflurane than N_2O in both the gas and blood phases.

Table 1. Physiologic Variables in the Study Sample

Characteristic	Measured Value
Age, yr	66.2 (9.4)
Height, cm	169 (9)
Weight, kg	82.4 (14.2)
Tidal volume, ml	487 (68)
Respiratory rate, breaths/min	12.6 (0.9)
Peak inspiratory pressure, cm H_2O	19.0 (4.8)
Alveolar ventilation rate ($\dot{V}A$), l/min	3.9 (1.2)
Mean arterial pressure, mmHg	78.0 (9.7)
Heart rate, beats/min	66.6 (9.3)
Cardiac output ($\dot{Q}t$), l/min	4.0 (1.1)
Temperature, °C	35.8 (0.6)
Oxygen uptake rate (Fick, $\dot{V}O_2$), ml/min	166 (45)
CO_2 elimination rate (Fick, $\dot{V}CO_2$), ml/min	166 (52)
Shunt fraction ($\dot{Q}s/\dot{Q}t$ for O_2)	0.149 [0.118, 0.168]
Arterial CO_2 partial pressure $Paco_2$, mmHg	42.6 (5.5)
Alveolar deadspace fraction $V_D/V_T CO_2$	0.283 (0.044)

The physiologic variables were measured in the study sample (n = 17) at the time of sampling. The shunt fraction was calculated from blood oxygen content using the shunt equation ($\dot{Q}s/\dot{Q}t$ for O_2) and alveolar deadspace fraction calculated from CO_2 partial pressures using the Bohr–Enghoff equation ($V_D/V_T CO_2$) are also listed. The data are expressed as means (SD) for normally distributed variables and as medians [upper quartiles, lower quartiles] otherwise.

Table 2 also shows the comparison of the alveolar deadspace fractions $V_D/V_T G$ and $(P_{ET}G - PaG)/FIG$ of the two anesthetic gases using these measured variables. $(P_{ET}G - PaG)/FIG$ was smaller for desflurane than N_2O (mean [SD], 0.86 [0.37] *vs.* 1.65 [0.58]; difference [95% CI], 0.79 [0.44, 1.12]; $P < 0.0001$; see fig. 1). $V_D/V_T G$ was also significantly smaller for desflurane than N_2O (mean [SD], 0.49 [0.14] *vs.* 0.76 [0.080]; difference [95% CI], 0.27 [0.19, 0.35]; $P < 0.0001$).

The linear relationship of $\dot{V}G$ to $(P_{ET}G - PaG)/FIG$ from equation 3 is shown in figure 2 for desflurane and N_2O (solid lines). The two gases followed very similar relationships with a mean (SD) slope of 0.60 (0.16) for desflurane *versus* 0.58 (0.03) for N_2O (mean [95% CI]; difference, 0.02 [–0.08, 0.12]; $P = 0.668$). The points of the mean measured values for desflurane and N_2O in table 2 are indicated. The position of $(P_{ET}G - PaG)/FIG$ for desflurane

Table 2. Variables for Each Gas in the Study

Measured Variable	Desflurane	N_2O	*P* Value
FIG , %	1.95 [1.80, 2.58]	13.0 [8.9, 13.7]	< 0.001
PETG/FIG, mmHg	6.32 (0.20)	6.63 (0.18)	< 0.0001
PaG /FIG , mmHg	5.46 (0.48)	4.99 (0.66)	0.024
$P\bar{v}G$ /FIG, mmHg	3.77 (0.69)	3.90 (0.65)	0.596
λG	0.50 [0.48, 0.52]	0.55 [0.49, 0.57]	0.027
Effective λG	0.48 [0.47, 0.51]	0.47 [0.43, 0.50]	0.224
$\dot{V}G$ /FIG blood phase, ml/min	4.4 [3.5, 5.0]*	3.3 [1.9, 4.2]†	0.030
$\dot{V}G$ /FIG gas phase, ml/min	3.9 [3.6, 5.1]*	2.7 [2.4, 3.3]†	0.001
(PETG – PaG)/FIG, mmHg	0.86 (0.37)	1.65 (0.58)	< 0.0001
V_{DA} / V_AG	0.49 (0.14)	0.76 (0.08)	< 0.0001

The table shows the measured variables for each gas (G; desflurane and N_2O) in the study sample (n = 17). The data are expressed as means (SD) for normally distributed variables and as medians [upper quartiles, lower quartiles] otherwise. The statistical significance of the difference between the two gases (*P* value) is shown in the right-hand column. Inspired concentration (FIG, expressed as %), and alveolar or end-tidal (PETG) , arterial (PaG) , and mixed venous ($P\bar{v}G$) partial pressures scaled by FIG are shown. Alveolar deadspace fraction (V_{DA} / V_AG) for each gas is also shown, as is scaled end-tidal to arterial partial pressure difference: FIG (PETG - PaG)/FIG. The raw measured and effective blood–gas partition coefficient λG and the scaled lung gas uptake rate $\dot{V}G$ /FIG are listed, measured in the both gas and blood phases with statistical comparisons between-gas (right-hand column) and within-gas.

*P = 0.877 for desflurane. †P = 0.804 for N_2O.

adjusted for the effect of its higher measured $\dot{V}G$ /FIG is also shown and was close to that of N_2O. The broken line corresponds to the position of a 20% greater end-tidal–arterial partial pressure gradient (ΔPDG) for desflurane than for N_2O due to gas phase diffusion limitation that was the study hypothesis. PETG/FIG and PaG/FIG values calculated from equations A14 and A15 and adjusted for the difference between $\dot{V}G$ /FIG for desflurane and N_2O are given in table 3. The adjusted (PETG – PaG)/FIG for desflurane was less than the hypothesized value (1.62 [0.61] *versus* 1.98 [0.69] mmHg; P = 0.028; difference [95% CI], 0.35 [–0.66, –0.02]; P = 0.038; see table 3). The mean (SD) V_{DA} / V_AG for desflurane calculated using these adjusted partial pressures was 0.74 (0.09), which was similar to that measured for N_2O (difference [95% CI], 0.03 [–0.03, 0.04]; P = 0.361).

Discussion

While the contribution of diffusion limitation to lung gas exchange efficiency has been extensively studied with respect to the respiratory gases, there has been little attempt to look for evidence of diffusion limitation for volatile anesthetics. Large molecules such as these might be expected to have lower diffusibility both within the conducting airways and at the alveolar–capillary interface, which might measurably contribute to the end-tidal–arterial partial pressure gradients seen in most anesthetized patients. The presence of end-tidal–arterial partial pressure gradients for volatile anesthetics are generally ignored in routine clinical practice, where end-tidal concentration monitoring is relied on as an indicator of anesthetic delivery and depth, but when measured these values are typically found to be between 15 and 30% of end-tidal partial pressure.[11,12,17–19]

This study did not find a larger end-tidal–arterial partial pressure gradient or alveolar deadspace to support the hypothesis that desflurane suffers clinically significant gas-phase diffusion limitation to its uptake by the lung in anesthetized patients relative to nitrous oxide. In contrast, it was found that raw measurements of end-tidal–arterial partial pressure gradients, relative to inspired concentration, are much smaller for desflurane and lead to a calculation of a substantially smaller alveolar deadspace fraction for desflurane than nitrous oxide, despite similar effective blood–gas partition coefficients (fig. 1). A confounding factor that was considered in this study was the higher rate of lung gas uptake $\dot{V}G$ for desflurane, which is driven by its greater solubility in peripheral body tissues than N_2O.[16,20] The need to

Table 3. Adjusted End-tidal and Arterial Partial Pressures and Difference for Desflurane

Adjusted Variable	Desflurane	Hypothesized (N_2O + 20%)	*P* Value
PETG/FIG, mmHg	6.56 (0.20)		
PaG/FIG, mmHg	4.94 (0.62)		
PETG – PaG/FIG, mmHg	1.62 (0.61)	1.98 (0.69)	0.028
V_{DA} / V_AG	0.73 (0.11)		

End-tidal (PETG/FIG) and arterial (PaG) partial pressures and difference (PETG – PaG)/FIG (scaled for inspired concentration, FIG) for desflurane, adjusted for the effect of lung gas uptake rate, compared with the hypothesized threshold of 20% above the (PETG – PaG)/FIG measured for N_2O in table 2. The data are expressed as means (SD). The statistical significance of the difference between the two gases (*P* value) is shown in the right-hand column. The alveolar deadspace fraction (V_{DA} / V_AG) for desflurane calculated from these adjusted partial pressures is also shown.

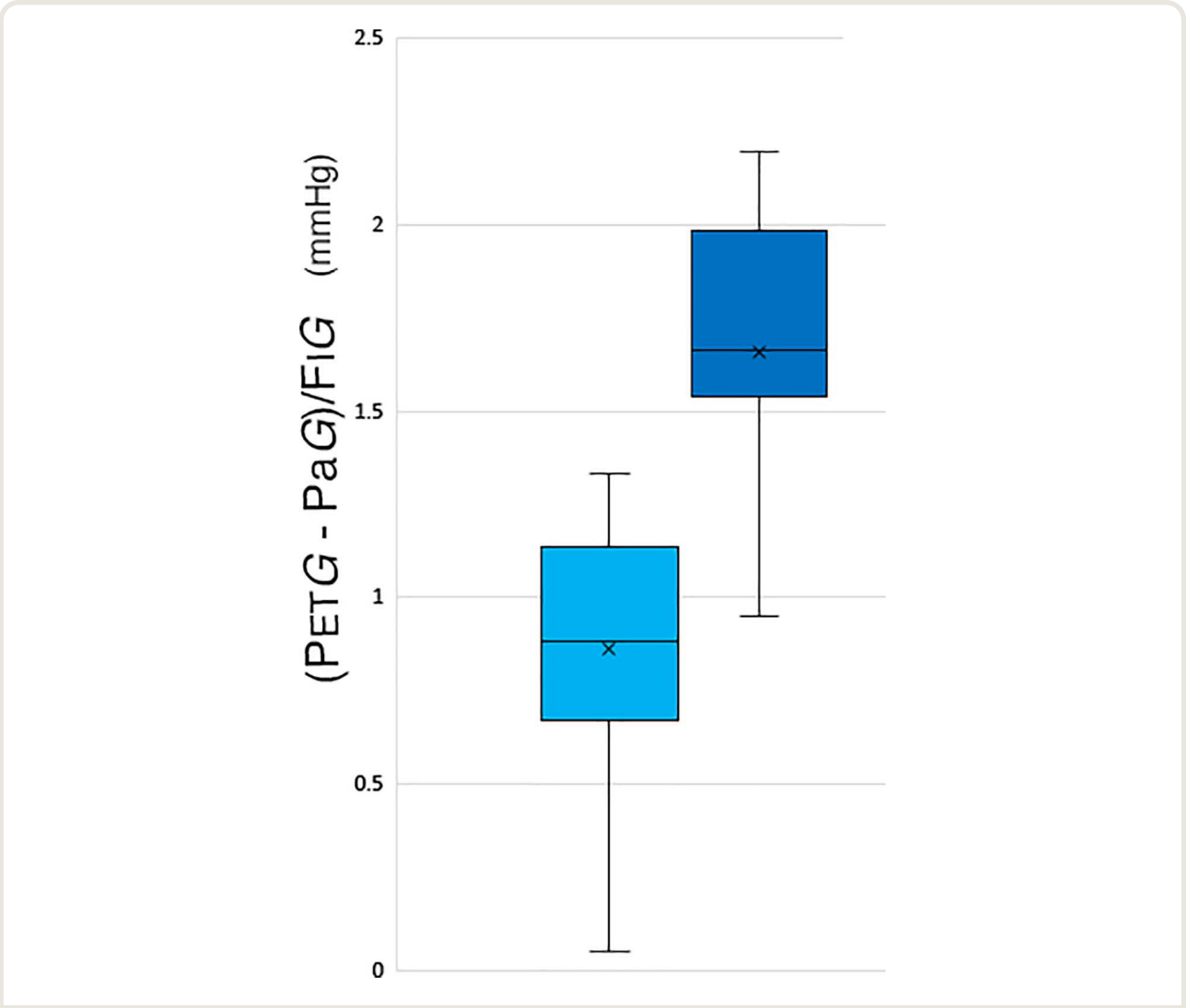

Fig. 1. Raw measured values for end-tidal–arterial partial pressure gradients (mmHg) scaled for inspired concentration (PETG – PaG)/FIG for desflurane (*light blue*) and N_2O (*dark blue*). *Crosses* show mean values, and *box-and-whisker plots* show medians and quartiles.

consider the rate of uptake of the two anesthetic gases being compared is a limitation in the study design, as it interferes with the assumptions made about similarity of the two gases in lung pharmacokinetics on the basis of their similar blood–gas partition coefficients. However, the potential effect of this on the measurements of end-tidal–arterial partial pressure gradients was able to be estimated from equation 3 and is shown graphically in figure 2. This indicates that, while the higher $\dot{V}G$ for desflurane is the primary driver of the smaller measured (PETG – PaG)/FIG and alveolar deadspace for desflurane than N_2O, the two gases follow closely aligned relationships due to their similar solubilities in blood and the paired data study design. Figure 2 and table 3 show that after adjustment for its $\dot{V}G$, which is higher than that of N_2O, the (PETG – PaG)/FIG value of desflurane remains virtually identical to that of N_2O and significantly below the point representing an hypothesized diffusion limited partial pressure gradient.

These findings for the behavior of a volatile anesthetic in an anesthetized population contrast with those of previous work using other gases, populations, and methodologies. Generation of larger concentration gradients for heavier gases is predicted by computer models of gas transport in the lung, and *in vivo* evidence of this has been demonstrated when the exhaled concentration gradient for heavy gases such as sulfur hexafluoride (molecular weight, 146) were compared to helium.[8–10] This has been confirmed experimentally in dog lung preparations. However, this work compared gases with larger differences in molecular weight than was done in the current study.[21]

The hypothesis of the current study has origins in the finding of a much larger end-tidal–arterial partial pressure

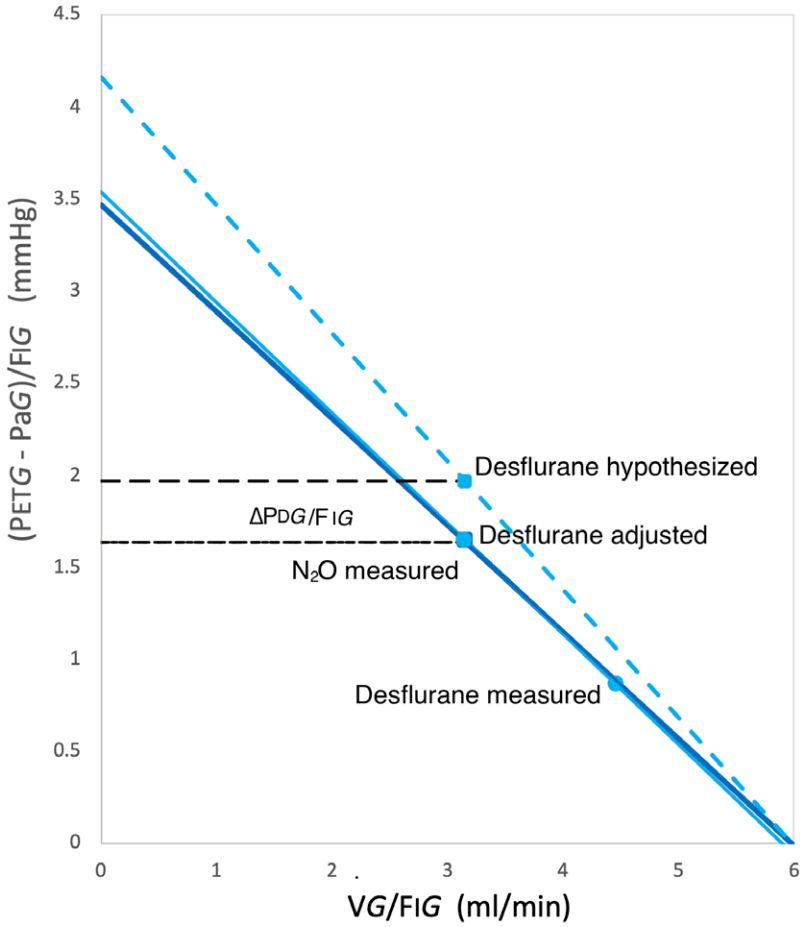

Fig. 2. The relationship of end-tidal–arterial partial pressure gradients (PETG – PaG)/FIG and lung gas uptake rate $\dot{V}G$ /FIG, both scaled for inspired concentration, for desflurane (*light blue*) and N_2O (*dark blue*), as described by equations 2 and 3. The points of the mean measured values for each gas shown in table 2 are indicated. The position of (PETG – PaG)/FIG for desflurane adjusted for the effect of its higher measured $\dot{V}G$ /FIG is also shown. The *broken line* corresponds to the position of the hypothesized 20% greater end-tidal–arterial partial pressure gradient for desflurane than for N_2O (ΔPDG/FIG) due to gas phase diffusion limitation.

gradient and alveolar deadspace for isoflurane than for carbon dioxide in anesthetized patients made by Landon *et al.*[11] almost three decades ago, which the authors suggested was potentially related to its larger molecular weight and lower diffusibility. Their proposition was in fact somewhat misplaced, because the authors confined their analysis to a traditional three compartment or Riley model of $\dot{V}_A / \dot{Q}$ scatter, which assumed that the alveolar deadspace for isoflurane would be identical to that measured for CO_2 using the Bohr–Enghoff equation. However, this conventional approach to calculation of alveolar deadspace for different gases has more recently been discredited. Peyton *et al.*[12] showed that estimates of alveolar deadspace by the Bohr–Enghoff equation using carbon dioxide measurements vastly underestimate the alveolar deadspace measured simultaneously using partial pressures of volatile anesthetic anesthetics, which have lower solubility in blood than carbon dioxide. This was explained by modeling realistic distributions of alveolar ventilation and blood flow in the lung, that showed the different positions of distributions of gas exchange across the lung for gases of different blood solubility in the presence of $\dot{V}_A / \dot{Q}$ scatter, resulting in different degrees of "wasted ventilation" and alveolar deadspace. Nevertheless, despite demonstrating that most of the differences in alveolar deadspace between gases of different solubilities is explained by the effect of $\dot{V}_A / \dot{Q}$ scatter, that study also raised the possibility of a residual, if modest contribution to the larger measured alveolar deadspace for volatile anesthetics, over and above the effect of $\dot{V}_A / \dot{Q}$ scatter alone, potentially related to their larger molecular weight and lower diffusibility.[12] The data in the current study and the relationships shown in equations 1 to 3 may explain this. A smaller alveolar deadspace for a highly soluble gas like CO_2 with a high rate of $\dot{V}G$ relative to its end-tidal–arterial partial pressure gradient is expected due to mass balance considerations alone (equation 1), without

any contribution from diffusion limitation, compared to less soluble anesthetic gases. Thus, this proposition, originally raised by Landon *et al.*[11] and pursued more recently by us[12] is refuted by the data collected in the current study. Indeed, the effect of $\dot{V}G$ has possibly been overlooked as a factor affecting predicted end-tidal–arterial partial pressure gradients and alveolar deadspace calculations for inspired gases.

This study was a small, single investigator study, and replication of these findings by other investigators would be useful. Incomplete data from 3 of the 20 recruited patients for the reasons stated precluded their inclusion in the final data set, but this is unlikely to have significantly changed the study findings. The need for adjustment of measured end-tidal–arterial partial pressure gradients for lung gas uptake rate was not preplanned but introduced after early interim examination of the raw data. The study methodology has other limitations in addition to these potential sources of bias. While the findings do not support a clinically significant contribution of diffusion limitation to end-tidal–arterial gradients and alveolar deadspace of desflurane due to the higher molecular weight, it is possible that this remains obscured by other factors. Alveolar ventilation rate ($\dot{V}_A$) was calculated using measurements of CO_2 and generalized to the two study anesthetic gases. While N_2O shares an identical molecular weight to CO_2, a different effective deadspace and $\dot{V}_A$ for desflurane to the other gases is a potential confounding factor in the adjustments made using the mass balance model in the Appendix. Similarly, another possibility is that the gas concentration present in the end-tidal (mixed alveolar) plateau of the expirogram may not reflect the presence of stratification in the distal airways. This may instead manifest as subtle differences in the shape or slope of the expirogram for gases of different diffusibility, that were not within the scope of the current study.

Furthermore, the use of two gases of similar blood solubility but different molecular weights was designed to identify any differences between desflurane and nitrous oxide in end-tidal to arterial partial pressure gradients due to longitudinal stratification in the gas phase, governed by Graham's law, and has been used in previous studies in the field.[22] However, this methodology is not as effectively designed to distinguish diffusion limitation at the level of the alveolar–capillary membrane, which is governed by a more complex mix of factors, including molecular diameter. Alveolar–capillary gas transfer has been extensively studied for the respiratory gases. Limitation to the rate of transfer from gas to blood of oxygen, which has very low solubility, is understood to occur at additional points to the alveolar–capillary membrane and include its diffusion into the erythrocyte and its interaction with hemoglobin, a more complex process, than is the case for inert gases. It is thought that significant contribution to oxygen alveolar–arterial partial pressure gradients from oxygen transfer limitation is not seen outside of exercise (with reduced pulmonary capillary transit time) and pulmonary pathology or edema.[23,24] In fact, most gas exchange impairment for oxygen in experimental studies of pulmonary edema is explained by $\dot{V}_A / \dot{Q}$ scatter rather than impaired conductance between gas and blood.[24,25] The greater solubility of carbon dioxide and the effect of carbonic anhydrase also act to promote nearly complete equilibration of carbon dioxide in the absence of lung pathology.[26,27] Soluble inert gases such as nitrous oxide rely on no chemical reactions to equilibrate blood and alveolar content and have been assumed to suffer little or none of any limitations to alveolar–capillary diffusion seen with oxygen and carbon dioxide in lung pathology.[26] However, little data on alveolar–capillary diffusion of volatile anesthetics has been available. While the current study is not designed to investigate this specifically, the narrower measured partial pressure gradient for desflurane suggests that, in this population, any contribution from additional factors such as this probably remains small.

In conclusion, in anesthetized ventilated patients, comparison of the partial pressure cascade for desflurane and nitrous oxide, with similar solubility in blood, found a significantly smaller end-tidal–to–arterial partial pressure gradient and alveolar deadspace for desflurane, despite the possibility of gas phase diffusion limitation due to its higher molecular weight. After adjustment for different rates of lung gas uptake between the two gases, there still remained no evidence of an additional end tidal to arterial partial pressure gradient attributable to diffusion limitation.

Research Support

Supported by project grant No. DJ17/006 from the Australian and New Zealand College of Anaesthetists Research Foundation (Melbourne, Australia).

Competing Interests

Dr. Peyton has received research consultancy payments from Maquet Critical Care/Getinge (Rastatt, Germany) for an unrelated project.

Correspondence

Address correspondence to Dr. Peyton: Austin Health, Studley Road, Heidelberg 3084, Victoria, Australia. phil.peyton@austin.org.au.

Appendix: Calculations and Equations

A simple model of whole lung (single compartment) gas exchange was used, based on global mass balance, for an inert gas (G) with no diffusion limitation, to calculate the expected mixed alveolar partial pressure (P_AG), and arterial partial pressure (PaG) of G, and therefore of ($P_AG - PaG$), and of alveolar deadspace fraction (V_{DA}/V_A) for a given set of measured input variables, incorporating oxygen uptake

($\dot{V}O_2$), carbon dioxide elimination ($\dot{V}CO_2$) and uptake of an inert gas ($\dot{V}G$), as follows:

Gas Exchange, Alveolar Ventilation Rate, and Shunt Fractions

$\dot{V}O_2$ was calculated from measured thermodilution cardiac output $\dot{Q}t$ using the Fick equation and from the measured values obtained on blood–gas analysis for arterial (CaO_2) and mixed venous ($C\bar{v}O_2$) blood oxygen content.

$$\dot{V}O_2 \times \dot{Q}t \times (CaO_2 - C\bar{v}O_2) \quad \text{Equation A1}$$

Shunt fraction ($\dot{Q}s / \dot{Q}t$) was calculated from measured O_2 content in blood using the shunt equation of Berggren.

$$\dot{Q}s / \dot{Q}t = \frac{Cc'O_2 - CaO_2}{Cc'O_2 - C\bar{v}O_2} \quad \text{Equation A2}$$

End-capillary oxygen content $Cc'O_2$ was obtained from estimated O_2 partial pressure using the alveolar gas equation and the equations of Kelman, which estimate O_2 hemoglobin saturation from partial pressure.[27]

Similarly, $\dot{V}CO_2$ was calculated from arterial ($CaCO_2$) and mixed venous ($C\bar{v}CO_2$) blood CO_2 content obtained from measured PCO_2, pH, hemoglobin O_2 saturation, and bicarbonate concentration in arterial and mixed venous blood according to the equations of Kelman.[28,29]

$$\dot{V}CO_2 = \dot{Q}t \times (C\bar{v}CO_2 - CaCO_2) \quad \text{Equation A3}$$

$\dot{V}A$ was then calculated from $\dot{V}CO_2$ and the measured end-tidal CO_2 partial pressure $PETCO_2$, which was used as a substitute for alveolar CO_2 partial pressure

$$\dot{V}A = \dot{V}CO_2 \times PB/PETCO_2 \quad \text{Equation A4}$$

where PB is barometric pressure. Note that equation A4 assumes no gas phase diffusion limitation and therefore no difference between end-tidal and alveolar partial pressure for CO_2. A similar assumption is implied in the study for N_2O, which has an identical molecular weight to CO_2.

For each of the two inert anesthetic gases (G) being studied (desflurane and N_2O), the rate of lung uptake of each gas $\dot{V}G$ measured in the blood phase was calculated similarly according to the Fick equation, from measured arterial (PaG) and mixed venous ($P\bar{v}G$) partial pressures and their respective blood–gas partition coefficients λG.

$$\dot{V}G = \dot{Q}t \times \lambda G \times (PaG - P\bar{v}G)/PB \quad \text{Equation A5}$$

$\dot{V}G$ values for desflurane and N_2O were also calculated in the gas phase from measured inspired partial pressure (PIG) and alveolar or end-tidal partial pressure ($PETG$),

$$\dot{V}G = (\dot{V}AI \times PIG - \dot{V}A \times PAG)/PB \quad \text{Equation A6}$$

where $\dot{V}AI$ is inspired alveolar ventilation rate and

$$\dot{V}AI = \dot{V}A + \dot{V}G + \dot{V}O_2 - \dot{V}CO_2 \quad \text{Equation A7}$$

so that

$$\dot{V}G = \frac{\dot{V}A \times (PIG - PAG) + (\dot{V}O_2 - \dot{V}CO_2) \times PIG}{PB - PIG} \quad \text{Equation A8}$$

Alveolar Deadspace

The alveolar deadspace fraction (VDA/V_A) was calculated from measured CO_2 partial pressures ($VDA/V_A\ CO_2$) using the Bohr–Enghoff equation, where arterial CO_2 partial pressure ($PaCO_2$) is used as an approximation of ideal alveolar CO_2 partial pressure.

$$VDA/VA\,CO_2 = \frac{PACO_2 - PaCO_2}{PICO_2 - PaCO_2} \quad \text{Equation A9}$$

Similarly, the alveolar deadspace $VDA/VA\ G$ for desflurane and N_2O were calculated according to the same mixing principle from measured variables.

$$VDA\ /\ VA\,G = \frac{PAG - PaG}{PIG - PaG} \quad \text{Equation A10}$$

Diffusion Limitation and End-tidal–to–Alveolar Partial Pressure Gradients

Equations A6 and A8 to A10 are modified where a diffusion related partial pressure gradient (ΔPDG) is postulated between measured end-tidal partial pressure ($PETG$) and PAG.

$$PAG = PETG - \Delta PDG \quad \text{Equation A11}$$

If ΔPDG is assumed to be 0, the end-tidal and alveolar partial pressures are considered identical for the purposes of the model.

Relationship of $\dot{V}G$ to ($PAG - PaG$) and $VDA\ /\ VA\,G$

The model was used to estimate the effects of the measured differences in $\dot{V}G$ between desflurane and N_2O on the comparison of ($PAG - PaG$) and $VDA\ /\ VA\,G$ for the two gases. For the alveolar deadspace fraction, transposing equation A8 and assuming that $PAG = PETG$

$$PIG - PETG = \frac{\dot{V}G \times (PB - PIG) - (\dot{V}O_2 - \dot{V}CO_2) \times PIG}{\dot{V}A} \quad \text{Equation A12}$$

If equation A10 is rewritten, then

$$VDA/VA\,G = \frac{PETG - PaG}{PIG - PETG + PETG - PaG} \quad \text{Equation A13}$$

Substituting the right hand term in equation A12 in it shows that alveolar deadspace fraction $VDA/VA\ G$ becomes a function of $\dot{V}G$

$$VDA/VA\,G = \frac{PETG - PaG}{\frac{\dot{V}G \times (PB - PIG) - (\dot{V}O_2 - \dot{V}CO_2) \times PIG}{\dot{V}A} + PETG - PaG} \quad \text{Equation 1}$$

Alveolar–arterial Partial Pressure Gradients

With alveolar–arterial partial pressure gradients, transposing equation A5, we get

$$PaG = P\bar{v}G + \dot{V}G \times PB/(\dot{Q}t \times \lambda G) \quad \text{Equation A14}$$

and from equation A8, assuming that $P_AG = P_{ET}G$.

$$P_{ET}G = P_IG - \frac{\dot{V}G \times (PB - P_IG) - (\dot{V}O_2 - \dot{V}CO_2) \times P_IG}{\dot{V}_A} \quad \text{Equation A15}$$

Combining equations A14 and A16 and considering that $P_IG = F_IG \times PB$,

$$(P_{ET}G - PaG)/F_IG = PB \times \left(1 + \frac{\dot{V}O_2 - \dot{V}CO_2}{\dot{V}_A}\right) \quad \text{Equation (2)}$$
$$- \frac{P\bar{v}G}{F_IG} - \frac{PB \times \dot{V}G}{F_IG} \times \left(\frac{\dot{V}_A + \dot{Q}t \times \lambda G \times (1 - F_IG)}{\dot{V}_A \times \dot{Q}t. \times \lambda G}\right)$$

The slope of the effect of a change in $\dot{V}G$ on $(P_{ET}G - PaG)/F_IG$ is obtained by differentiation of $(P_{ET}G - PaG)/F_IG$ with respect to $\dot{V}G$, treating the other variables as independent.

$$\frac{d(P_{ET}G - PaG)/F_IG}{d\dot{V}G/F_IG} = - PB \times \left(\frac{\dot{V}_A + \dot{Q}t \times \lambda G \times (1 - F_IG)}{\dot{V}_A \times \dot{Q}t. \times \lambda G}\right) \quad \text{Equation 3}$$

References

1. Scheid P, Hlastala MP, Piiper J: Inert gas elimination from lungs with stratified inhomogeneity theory. Respir Physiol 1981; 44:299–309
2. Lundh R, Hedenstierna G: Ventilation–perfusion relationships during anaesthesia and abdominal surgery. Acta Anaesthesiol Scand 1983; 27:167–73
3. Lundh R, Hedenstierna G: Ventilation–perfusion relationships during halothane anaesthesia and mechanical ventilation: Effects of varying inspired oxygen concentration. Acta Anaesthesiol Scand 1984; 28:191–8
4. Hedenstierna G, Lundh R, Johansson H: Alveolar stability during anaesthesia for reconstructive vascular surgery in the leg. Acta Anaesthesiol Scand 1983; 27:26–34
5. Dueck R, Young I, Clausen J, Wagner PD: Altered distribution of pulmonary ventilation and blood flow following induction of inhalation anesthesia. Anesthesiology 1980; 52:113–25
6. Bindislev L, Hedenstierna G, Santesson J, Gottlieb I, Carvallhas A: Ventilation–perfusion distribution during inhalation anaesthesia. Acta Anaesth Scand 1981; 25:360–71
7. Rehder K, Knopp TJ, Sessler AD, Didier EP: Ventilation–perfusion relationship in young healthy awake and anesthetized–paralyzed man. J Appl Physiol Respir Environ Exerc Physiol 1979; 47:745–53
8. Paiva M: Gas transport in the human lung. J Appl Physiol 1973; 35:401–10
9. Piiper J, Scheid P: Blood–gas equilibration in lungs, Pulmonary Gas Exchange. Edited by West JB, New York, Academic Press Publishers, 1980, pp 131–71
10. Scheid P, Piiper J: Intrapulmonary gas mixing and stratification, Pulmonary Gas Exchange. Edited by West JB, New York, Academic Press Publishers, 1980, pp 87–130
11. Landon MJ, Matson AM, Royston BD, Hewlett AM, White DC, Nunn JF: Components of the inspiratory–arterial isoflurane partial pressure difference. Br J Anaesth 1993; 70:605–11
12. Peyton PJ, Hendrickx J, Grouls RJE, Van Zundert A, De Wolf A: End-tidal to arterial gradients and alveolar deadspace for anesthetic agents. Anesthesiology 2020; 133:534–47
13. Peyton PJ, Chong M, Stuart-Andrews C, Robinson GJ, Pierce R, Thompson BR: Measurement of anesthetics in blood using a conventional infrared clinical gas analyzer. Anesth Analg 2007; 105:680–7
14. Eger EI 2nd, Smith RA, Koblin DD: The concentration effect can be mimicked by a decrease in blood solubility. Anesthesiology 1978; 49:282–4
15. West JB, Wagner PD, Derks CM: Gas exchange in distributions of VA–Q ratios: Partial pressure–solubility diagram. J Appl Physiol 1974; 37:533–40
16. Eger EI: Uptake and distribution, Miller's Anaesthesia, 4th edition. Edited by Miller RD, Philadelphia, Elsevier Churchill Livingston, 1990, pp 102–4
17. Frei FJ, Zbinden AM, Thomson DA, Rieder HU: Is the end-tidal partial pressure of isoflurane a good predictor of its arterial partial pressure? Br J Anaesth 1991; 66:331–9
18. Dwyer RC, Fee JP, Howard PJ, Clarke RS: Arterial washin of halothane and isoflurane in young and elderly adult patients. Br J Anaesth 1991; 66:572–9
19. Peyton PJ, Horriat M, Robinson GJ, Pierce R, Thompson BR: Magnitude of the second gas effect on arterial sevoflurane partial pressure. Anesthesiology 2008; 108:381–7
20. Lowe HJ, Viljoen JF: Nomogram for anaesthetic uptake. Anaesth Intensive Care 1994; 22:374–5
21. Okubo T, Piiper J: Intrapulmonary gas mixing in exercised dog lung lobes studied by simultaneous wash-out of two inert gases. Respir Physiol 1974; 21:223–39
22. Neufeld GR, Gobran S, Baumgardner JE, Aukburg SJ, Schreiner M, Scherer PW: Diffusivity, respiratory rate and tidal volume influence inert gas expirograms. Respir Physiol 1991; 84:31–47
23. Hopkins SR, McKenzie DC, Schoene RB, Glenny RW, Robertson HT: Pulmonary gas exchange during exercise in athletes: I. Ventilation–perfusion mismatch and diffusion limitation. J Appl Physiol (1985) 1994; 77:912–7
24. Yamaguchi K, Kawai A, Mori M, Asano K, Takasugi T, Umeda A, Yokoyama T: Continuous

distributions of ventilation and gas conductance to perfusion in the lungs. Adv Exp Med Biol 1990; 277: 625–36
25. Coffey RL, Albert RK, Robertson HT: Mechanisms of physiological dead space response to PEEP after acute oleic acid lung injury. J Appl Physiol Respir Environ Exerc Physiol 1983; 55:1550–7
26. West JB: Respiratory Physiology: The Essentials, 4th edition. Baltimore, Williams & Wilkins, 1990, p 23
27. Nunn, JF: Diffusion and alveolar/capillary permeability, Applied Respiratory Physiology, 4th edition. Oxford, Butterworth–Heinemann, 1993, pp 211–4
28. Kelman GR: Digital computer subroutine for the conversion of oxygen tension into saturation. J Appl Physiol 1966; 21:1375–6
29. Kelman GR: Digital computer procedure for the conversion of PCO2 into blood CO^2 content. Respir Physiol 1967; 3:111–5

ANESTHESIOLOGY REFLECTIONS FROM THE WOOD LIBRARY-MUSEUM

Vesalius' *Fabrica*: Sublime Anatomy, Crude Physiology

Flemish physician Andreas Vesalius (1514 to 1564, *lower left*) relished dissecting cadavers and inspecting cemetery bones as a medical student at the University of Paris. By age 23, he was appointed Professor of Surgery and Anatomy at the University of Padua. A Paduan judge so admired his work that he began supplying him with bodies of executed criminals for examination. Vesalius soon found anatomic errors in the long-revered texts of Galen (129 to c. 216 CE), who by Roman imperial decree had only been allowed to dissect animals. Vesalius published his magnificent *De humani corporis fabrica* (*upper middle*), or simply, the *Fabrica*, in 1543, the same year as Copernicus' *On the Revolutions of the Celestial Spheres*. Although best known for the sublime detail of its anatomic illustrations, the *Fabrica* also contained decorative initials with mischievous *putti*, chubby child figures, in morbid scenes. Through these crude images, Vesalius paid homage to Galen's use of live animal dissection to learn physiology. In the book's preface, a large letter Q featured *putti* vivisecting a restrained pig's neck (*lower right*). After lecturing on the anatomy of the recurrent laryngeal nerves, Vesalius repeated Galen's experiment by cutting the nerves of a pig to abolish its squeal. (Lanska DJ. *J Hist Neurosci* 2014; 23:211–32. Copyright © the American Society of Anesthesiologists' Wood Library-Museum of Anesthesiology. www.woodlibrarymuseum.org)

Jane S. Moon, M.D., Assistant Clinical Professor, Department of Anesthesiology and Perioperative Medicine, University of California, Los Angeles, California.